DEVELOPMENT OF CUTTING TOOL THROUGH SUPERPLASTIC DEFORMATION METHOD ON BORONIZED DUPLEX STAINLESS STEEL

MAZLAN BIN SHAH

FACULTY OF ENGINEERING
UNIVERSITY OF MALAYA
KUALA LUMPUR

2013

DEVELOPMENT OF CUTTING TOOL THROUGH SUPERPLASTIC DEFORMATION METHOD ON BORONIZED DUPLEX STAINLESS STEEL

MAZLAN BIN SHAH

DISSERTATION SUBMITTED IN PARTIAL FULFILLMENT OF
THE REQUIREMENTS FOR THE DEGREE OF
MASTER OF ENGINEERING

FACULTY OF ENGINEERING
UNIVERSITY OF MALAYA
KUALA LUMPUR

2013

UNIVERSITY OF MALAYA

ORIGINAL LITERARY WORK DECLARATION

Name of Candidate: MAZLAN BIN SHAH
I.C. No.:
Matric No.: KGG090002

Name of Degree: MASTER OF ENGINEERING

Title of Dissertation ("this Work"):

DEVELOPMENT OF CUTTING TOOL THROUGH SUPERPLASTIC DEFORMATION METHOD ON BORONIZED DUPLEX STAINLESS STEEL
Field of Study: ADVANCED MATERIALS

I do solemnly and sincerely declare that:

(1) I am the sole author/writer of this Work;
(2) This Work is original;
(3) Any use of any work in which copyright exists was done by way of fair dealing and for permitted purposes and any excerpt or extract from, of reference to or reproduction of any copyright work has been disclosed expressly and sufficiently and the title of the Work and its authorship have been acknowledged in this Work;
(4) I do not have any actual knowledge nor ought I reasonably to know that the making of this work constitutes an infringement of any copyright work;
(5) I hereby assign all and every rights in the copyright to this Work to the University of Malaya ("UM"), who henceforth shall be owner of the copyright in this work prohibited without the written consent of UM having been first had and obtained;
(6) I am fully aware that if in the course of making this Work I have infringed any copyright whether intentionally or otherwise, I may be subject to legal action or any other action as may be determined by UM.

Candidate's Signature Date

Subscribed and solemnly declared before,

Witness's Signature Date

Name:
Designation:

ABSTRACT

In this study, focus was set upon developing new method to produce cutting tool through the employment of superplastic boronizing and duplex stainless steel, within which formation of the cutting tool from boronized duplex stainless steel subjected to superplastic deformation was tested against the determining parameters, strain and strain rate. As received DSS specimen was thermo-mechanically treated by heating up to 1537K, holding for one hour, followed by water quenching and then cold rolled to a plate through a reduction area of 75%. Prior to superplastic forming, treated DSS was boronized at 1223K for 6 hours, thereafter producing average surface hardness of 2247 HV and layer thickness of 46.3 µm. Then, the specimen was superplastically deformed into designated cutting tool at 1223K with the strain rate of $1x10^{-4}$ and $9x10^{-5}$ s^{-1}. Result showed that the flow stress of the deformed specimen was higher at the faster strain rate. At slower strain rate and low strain (0.4), no flaws were observed at the surface of the deformed specimen. However, at faster strain rate and higher strain (0.8 and 1.0) flaws that lead to surface disintegration were observed. It is very crucial to control these parameter (strain rate and strain) to avoid any surface flaw (disintegrity) to the specimen.

ABSTRAK

Dalam kajian ini, superplastic boronizing dan keluli tahan karat duplek telah dimanfaatkan untuk pembangunan kaedah baru dalam menghasilkan alat pemotong. Penghasilan alat pemotong melalui ubah bentuk superplastic terhadap keluli tahan karat duplek terboron telah dikaji dengan menggabungkan beberapa set parameter terikan dan kadar terikan. Specimen DSS telah dirawat secara mekanikal-haba dengan memanaskannya hingga 1573K, ditahan selama 1 jam, diikuti dengan lindap kejut air dan dicanai dingin kepada kepingan dengan kadar pengurangan ketebalan sebanyak 75%. Proses pemboronan dilakukan pada suhu 1223K selama 6 jam yang mana menghasilkan kekerasan permukaan 2247HV dan ketebalan lapisan terboron sebanyak 46.3 µm. Spesimen kemudiannya dibentuk menjadi cutting tool yang dikehendaki secara superplastik pada suhu 1223K dengan kadar terikan $1x10^{-4}$ and $9x10^{-5}$ s^{-1} . Keputusan menunjukkan aliran tegasan terhadap specimen yang di bentuk adalah tinggi pada kadar terikan yang lebih tinggi. Pada kadar terikan dan terikan (0.4) yang rendah, telah diperhatikan tiada kecacatan pada permukaan specimen. Walau bagaimanapun, pada kadar terikan and terikan (0.8, 1.0) yang tinggi telah diperhatikan kehadiran kecacatan yang menyebabkan disintegriti permukaan. Adalah sangat penting mengawal parameter (aliran tegasan, kadar terikan and terikan) untuk mengelakkan sebarang kecacatan permukaan (disintegriti) terhadap specimen.

ACKNOWLEDGEMENT

Thank you Almighty Allah for the good health, strength, patience and thought bestowed upon me in accomplishing my master of engineering degree and this dissertation.

I would like to express my deepest appreciation to my supervisor, Dr. Iswadi Jauhari for giving me the opportunity to do this research. I truly value his guidance, supervision, encouragement, time spent, valuable knowledge and experience shared.

I owe my heartfelt gratitude to my fellow colleagues, Hasanuddin Ismail, Rosnaini Saidan for their help and continuous support. Appreciation also extended to all lecturers, staff of Engineering Faculty, University of Malaya for the contribution rendered in every respect during the completion of this research.

My beloved family, too, deserve special mention commemorating their undivided supports and prayers. My lovely wife, first and foremost, Noriame Ahmad, for never failing to give me wonderful support and care through this scholarly journey; my mother, Habesah Badiozaman, for raising me sincerely and the wisdom in her counsel always; my brothers and sister, thanks for being supportive and caring.

I would also like to thank everybody especially my friends in honour of their remarkable encouragements in pursuing my master degree, and I suppose an apology is duly for not being able to mention them individually.

TABLE OF CONTENTS

LIST OF FIGURES

Figure **Captions** **Page**

LIST OF TABLES

Table **Caption** **Page**

LIST OF SYMBOLS AND ABBREVIATIONS

Symbols	Explanation
M	Strain-rate sensitivity
σ	plastic flow stress
F	applied force
A	cross-sectional area
K	constant

Abbreviations	Explanation
SEM	Scanning electron machine
EDX	Energy dispersive X-ray
GBS	Grain boundary sliding
FSS	Fine-structure superplasticity
ISS	Internal-stress superplasticity
T_m	Melting temperature
M	High strain-rate sensitivity
SPD	Superplastic deformation
SPF	Superplastic forming
DB	Diffusion bonding

CHAPTER 1

1. INTRODUCTION

1.1. Superplasticity

Superplasticity is a phenomenon that allows materials to undergo extreme plastic elongation. Numerous researches directed on developing new alloys and material, process optimization and microstructural studies aimed to understand the fundamental mechanisms of this process.

A new surface hardening technique, *Superplastic Boronizing (SPB),* is derived from the said phenomenon in metals exercised in boronizing process. In this process, the boron atoms are diffused into the metal substrate to form a hard boride layer. The basic principle of superplastic boronizing is to conduct boronizing while the specimen is engaged in superplastic deformation. This process has a much faster boronizing rate as compared to the conventional boronizing process, and it also produces equi-axed boride grains with low growth texture instead of acicular grains after conventional boronizing. (C. H. Xu, Xi, & Gao, 1997)

In this research, high temperature compression is introduced to the SPB material to form a pressed cutting tool. From the experimental and industrial point of view, the process set up for compression method seen to be much easier rather than the tensile method as this will represent the same result. Many studies related to superplasticity boronizing (SPB) centred mostly on fundamental aspects such as surface hardness and boronized layer thickness. Outcomes of the preceding work were adopted as the

reference for this feasibility study on developing a cutting tool through superplastic deformation method of boronized duplex stainless steel.

Machining the materials for high performance workpiece demands a harder cutting counterpart. During tough machining, cutting tools are quick to deteriorate due to high forces and temperatures of the process. The hardest known material is the diamond, but steel materials cannot be machined with diamond tools because of the reactivity between iron and carbon. Cubic boron nitride (cBN) is the second hardest of all known materials. The supply of such PcBN indexable inserts, which are only geometrically simple and available, requires several work procedures and is cost-intensive. (Uhlmann, Fuentes, & Keunecke, 2009)

In most cases, cutting tools are coated by other materials to form high surface hardness, improve wear resistance and lifetime of the tool. Common methods used for coating are chemical vapor deposition (CVD) and physical vapor deposition (PVD). The purpose of the coating process is to improve the insert's lifetime and wear resistance. There are a number of drawbacks to CVD and PVD though, for instance, complexity of its procedure, costly, and applicable only to insert with uncomplicated shape. In addition, there are various quantifying aspects involved besides elaborated deposition process. Therefore, the findings from this research will be beneficial in both superplasticity and surface engineering area.

1.2. Objectives

The objectives of this study are:

1) To develop a new method to produce cutting tool which is more practical, economical and yet with superior properties for the specific niche application.

2) To study the feasibility of developing cutting tool through superplastic deformation method on duplex stainless steel.

1.3. Research Plan

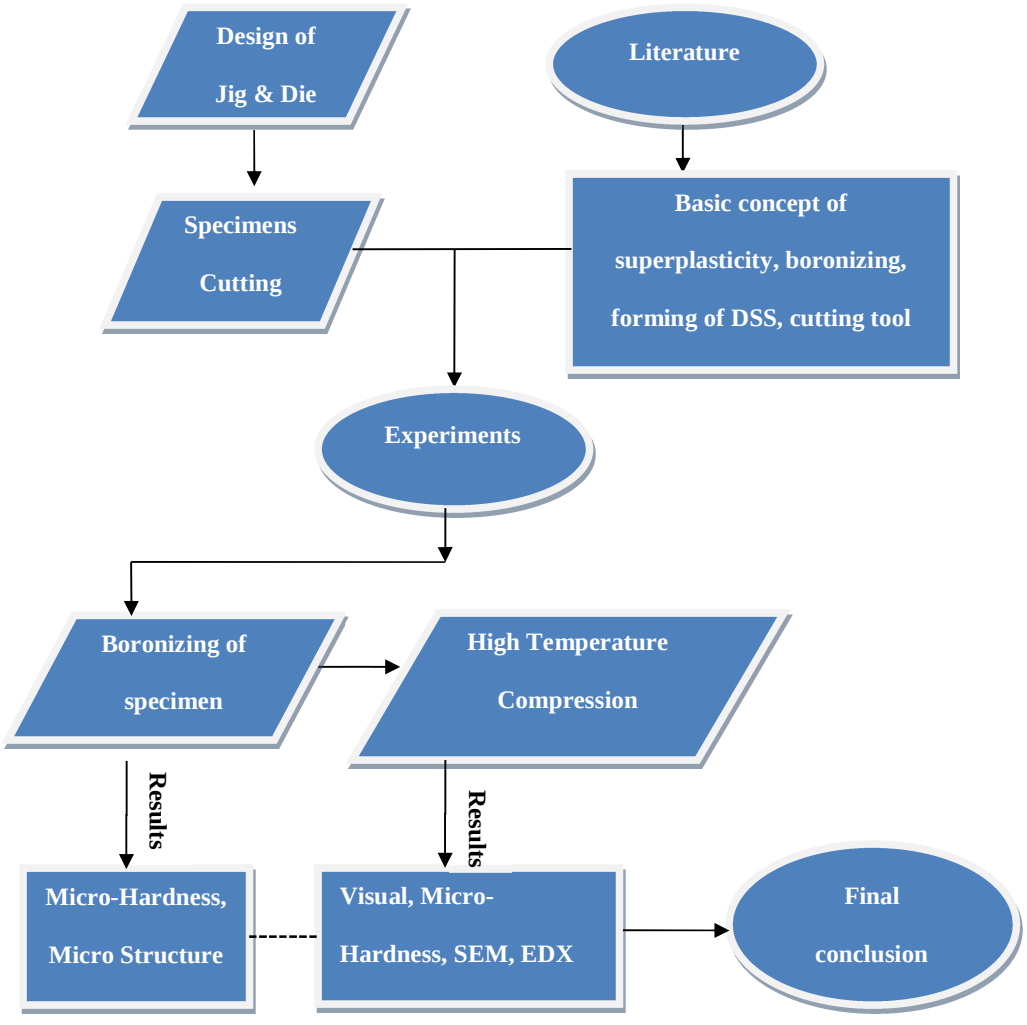

Figure 1.1 Framework and steps of the dissertation study

The order of chapters indicates the steps of the research and following procedures:

1. Literature review

The chapter starts with the preliminary definitions, the basic concepts of superplasticity, boronizing and superplastic boronizing were reviewed from various sources such as journal, previous dissertation reports, conference proceedings and world wide web.

2. Jig & Die Preparation & Experimental works

This involve designing jig & die, conducting superplastic boronizing experiments using fine microstructure duplex stainless steel and followed by superplastic forming using compression testing machine (Instron) equipped with high temperature furnace under controlled argon gas environment.

3. Characterization

Hardness before and after boronizing were measured using vicker microhardness tester. Thickness measurement and microstructure evaluation were done using optical microscope and scanning electron microscope (SEM). The presence of borides on the surface of the boronized specimens was determined by using Energy Dispersive X-ray Spectroscope (EDX).

4. Data collection and data analysis

Data from characterization process were collected and further analyzed to identify duplex stainless steel behavior under high temperature forming and estimate the optimum forming parameters for future reference in its evolution.

5. Discussion & Recommendation

All of the results obtained in this research were consolidated and discussed in chapter 4. Conclusion and recommendation for further improvement were presented in chapter 5.

CHAPTER 2

2. LITERATURE REVIEW

2.1. Superplasticity

Superplasticity in duplex stainless steels was reported as early as 1967 and yet there has been no attempt to superplastically form these materials (Patankar, Lim, & Tan, 2000). Superplasticity can also be defined as a phenomenon of metals that can show a very large plastic deformation at high temperature. The high ductility achieved through superplastic materials is exploited to form components with complex shapes (Jauhari, Yusof, & Saidan, 2011). Superplastic materials exhibit very large elongations that are equal to or greater than 500% (in a special case, ≥5,000%). However, large elongations are usually attained only in a low strain- rate range of 10–5–10–3 s–1 (Mabuchi & Higashi, 1998).

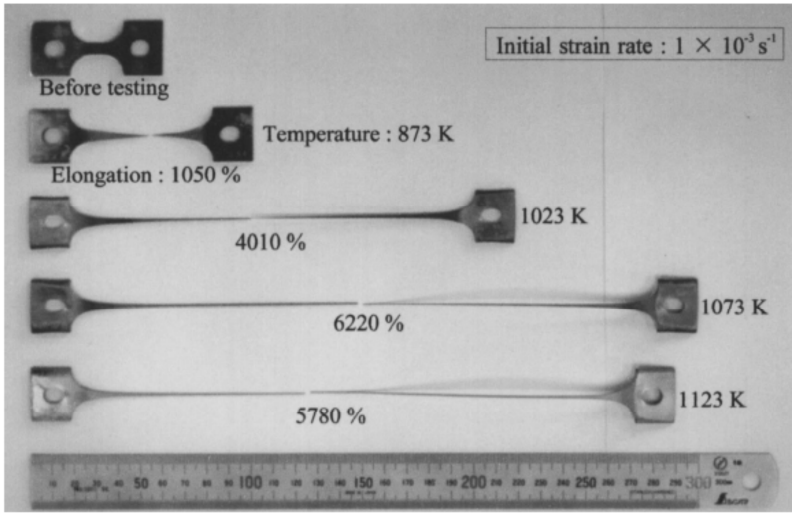

Figure 2.1 Appearance of superplastic elongated specimens of ultra-fine grained materials at various test temperatures (Nakahigashi & Yoshimura, 2002)

Superplasticity represents an inelastic behavior with high strain rate sensitivity, grain switching and grain boundary sliding (GBS). In superplastic material, grains remain nearly equiaxed even after deformation so it can be concluded that the primary mechanism in superplasticity is grain boundry sliding (Chandra, 2002; Vetrano, 2001). As shown in Figure 2.2, in superplasticity the grains change their neighbors and the original structure is restored. Through grain boundary sliding, the inelastic strain is produced (Chandra, 2002).

Generally there are two types of superplasticity: fine-structure superplasticity (FSS) and internal-stress superplasticity (ISS). FSS is considered as an internal structural feature of material and ISS is caused by special external conditions (e.g. thermal or pressure cycling) generating internal structural transformations that produce high internal stresses independent of external stresses.

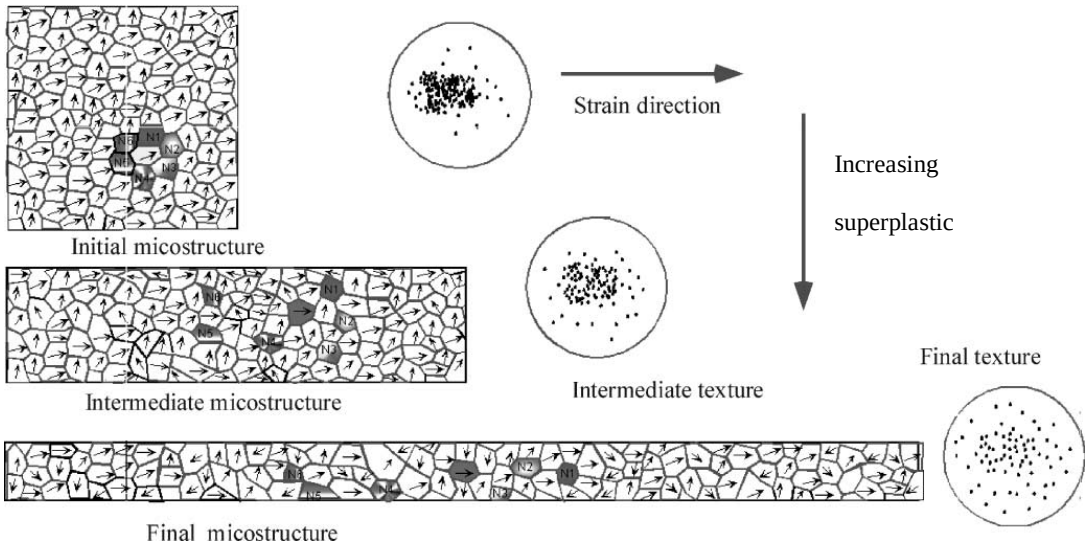

Figure 2.2 Evolution of microstructure during superplastic deformation (Chandra, 2002)

2.1.1. Historical Background of Superplasticity

Observation of alloys such as tin/lead and cadmium/zinc displayed abnormally high elongation under low loads and has been known since the early 1920s (Coiley, 1974). In 1934, Pearson did the earliest amazing observations on Bi-Sn eutectic alloy with a tensile elongation of 1950% without failure (Langdon, 2009). He also showed that the dimensions of the grains of the superplastic alloys, namely the size and shape, did not change during deformation. Following this observations, many researches related with superplastic were done.

2.1.2. Characteristics of Superplastic Deformation

There are several requirements for materials to exhibit superplasticity. Three main requirements for superplasticity: (1) deformation temperature > 0.5 T_m (where T_m is the absolute melting point) (2) fine equiaxed grains (3) high strain-rate sensitivity, *m* (typically close to 0.5) (Hertzberg, 1996)

2.1.3. Temperature

Temperature is considered to be one of the most important parameters in superplastic deformation as superplastic behaviour related with the movement of matter in general. And the displacement of matter such as the movement of gas particles, solid particles and water particles is a temperature dependent mechanism. In most materials, superplasticity commonly occurs at elevated temperature. Therefore any kind of method or process that is conducted at elevated temperature and contain deformation process can be used as a tool to study superplasticity mechanism.

The deformation temperature for superplasticity should be about half of the melting temperature; for titanium alloys this is about 90% of the β-transus temperature. Plastic deformation at these high temperatures is primarily due to creep. For favor creep deformation, two metallurgical properties are required: (1) extremely fine microstructures, because creep is primarily controlled by grain boundary sliding and (2) stability of the fine structures at the high deformation temperatures (Leyens & Peters, 2003).

2.1.4. Fine Grain size

As mentioned earlier, in superplastic deformation, microstructure plays an important role. A fine-grained equiaxed microstructure (grain size approximately <10μm) is needed for superplastic behavior. Apart from that, the structure must be resistant to grain growth at temperature and time during superplastic deformation (Courtney, 2000).

Recent experiments on microstructural processes occurring during superplastic deformation (Nieh *et al*., 1997; Mukherjee, 2002; Kaibyshev, 2002) proved existence of cooperative grain-boundary sliding related to sliding of groups of grains (Figure 2.3). It was found that operation of that mechanism does not depend on crystal lattice type and dislocation activity in grains. Occurrence of cooperative GBS is conditioned mainly by structure of grain boundaries in polycrystal. It was determined that cooperative GBS is also connected with rotation and migration of whole grain assemblies.

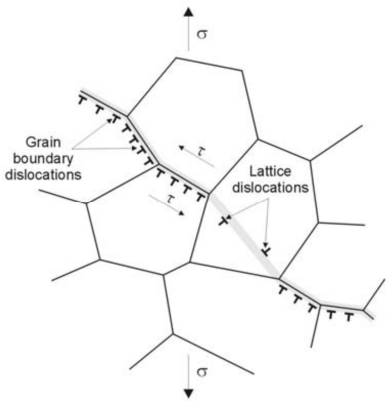

Figure 2.3 Grain boundary sliding (GBS) during superplastic deformation (Kaibyshev, 2002)

Other than that, it is difficult to observe superplasticity in single phase materials with very fine grain because grain growth is too rapid when it reaches the temperature at which grain boundary sliding occurs. Existence of second phase or presence of particles at grain boundaries is required to prevent the grain growth during superplastic deformation. Inhibition of grain growth is usually improved if the quantity of the second phase is increased, provided that the size of the second phase is fine and distribution is uniform (Nieh & Wadsworth, 1998).

2.1.5. Strain-rate sensitivity

High strain-rate sensitivity (typically close to 0.5) is one important factor in superplastic deformation which stabilizes against localized necking and results in high plastic elongation (Chandra, 2002; Vetrano, 2001). Different materials demonstrate different sensitivity on the strain rate and it depends on the structure of the material. The strain-rate sensitivity factor or the *m*-value in the well known flow stress-strain relation is shown in Equation (2.1).

$$\sigma = \frac{F}{A} = K\dot{\varepsilon}^{m}$$

where σ = plastic flow stress

F = applied force

A = cross-sectional area

K = constant

$\dot{\varepsilon} = \frac{1}{l}\frac{dl}{dt} = -\frac{1}{A}\frac{dA}{dt}$ = strain-rate

m = strain-rate sensitivity factor

The slope = $\partial(\ln \sigma) / \partial(\ln \dot{\varepsilon})$ represents the strain-rate sensitivity parameter (Figure 2.4) (Chandra, 2002). There is a slow strain-rate in Region 1 where the deformation occurs due to diffusion and grain coarsening is hindered (Leyens & Peters, 2003). Superplastic deformation is found in Region 2 with *m*-value more than 0.4. Region 3 is a high strain-rate region where the deformation occurs due to dislocation creep. This is where plastic deformation occurs with the elongated grains during the deformation.

In superplastic deformation (SPD) process, *m* is a critical parameter. With higher value of *m*, we will get higher values for superplastic properties (large elongation). Theoretically it can be shown that *m* is resistance to necking and during the deformation it provides more diffused necking, prolonging the stretching process (Chandra, 2002).

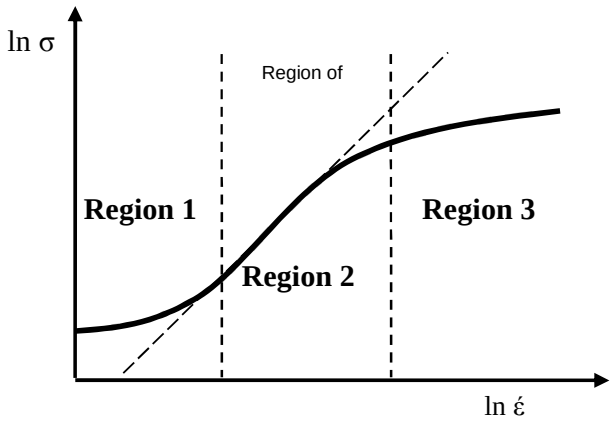

Figure 2.4 Stress-strain rate behavior of superplastic material (Hertzberg, 1995)

2.2. Applications of Superplasticity

Superplasticity has been developed and implemented in many industrial applications. Most of them are used to form parts in the automotive, aerospace and various other smaller industries. Superplastic forming (SPF) refers to a metal forming process that takes advantage of the metallurgical phenomenon of superplasticity to form complex shapes. Advantages of the process include reduced weight and part count as well as lower die costs which will be beneficial in producing aircraft components (Martin & Evans, 2000).

The SPF is conducted under controlled temperature and stain rates, drastically increasing the formability of materials and allowing production of which required extensive integration that often consolidates many parts into one. SPF process can

influence the strain of titanium SP-700 being employed in an elevated-temperature tensile test. This alloy can exhibit excellent superplastic characteristics at 1073 K. The lower forming temperature of this material lengthens tool life and eliminates the need for nitric-hydrofluoric acid chemical cleaning (Sanders & Ramulu, 2004). Emergency door for BAe 125 airplane produced from aluminium alloy using conventional methods is composed of 80 detail pressings and about 1000 fasteners. Fabrication of the same product from titanium alloy using SPF enables reduction of the large parts number to 4 and fasteners number to 90. It gives a cost saving of 30% overall (Demaid, 1992).

Superplastic forming (SPF) combined with diffusion bonding (DB) has been used successfully for the fabrication of titanium aerospace hardware. The process uses the two unusual properties of titanium alloys, superplasticity and diffusion bond ability which results in significant saving of cost and weight when compared to conventional titanium manufacturing methods (Wenbo *et al.*, 2007). Some of the primary applications for titanium SPF/DB are landing gear doors, engine fan blades, engine nacelles, auxiliary power unit thermal protection, environmental control system ducting and fuselage tunnel covers. Application of SPF/DB for producing aft fuselage of F-15E fighter allowed eliminating 726 parts and about 10,000 fasteners costs (Martin & Evans, 2000).

2.3. Boronizing

Boronizing is known in enhancing wear resistance of ferreous and non-ferreous substance. Boronizing is a thermo-chemical surface treatment process which involves atom diffusion onto the surface material to form boride layer that can give high surface hardness to the material. The hardness can exceed 2000 HV, better in strength to

friction wear and abrasion compared to carburizing and nitriding (Sinha, 1991). The thickness of boride layer formed is determined by the temperature and time of the treatment (Jain and Sundarajan, 2002). Boronizing typically requires process temperatures of 973 K to 1273 K in either gas, solid, or liquid media (Genel et al., 2003). Powder-pack boronizing was suggested by Keddam and Chentouf (2005) which has the advantages in the simplicity of the process and cost-effectiveness in comparison with other boronizing process.

In recent years, many studies had been carried out on the boronizing treatment. Most of the studies were based on the different material used being applied to the process and as a result explain the varying characterization of the surface coating obtained. Some other studies examined the effects of treatment parameters on the boronized surface, as well as the mechanical and the technological properties of these boronized materials.
Significant amount of research also has been done on the boronizing mechanism, acquisition of boriding layers and phase composition of boride layers. Keddam (2006) used computer simulation to explain development and transformation of phases of boride layer. On the other hand, Yu *et.al*. (2005) used numerical simulation to explain the same phenomenon.

Few researchers have worked on the surface roughness of boronizing material. Jain and Sundarajan (2002) found that the initial roughness of the steel sample prior to boronizing ranging from 0.2 to 0.3µm in *Ra,* and increased approximately by a factor of 2-3 with boronizing. The increase in roughness of the reasonably smooth surface was due to chemical reaction at the surface which resulting in the formation of iron borides. Yu *et al.* (2005) noted that the surface roughness of the sample increased during the boronizing process while investigation the growth kinetics of boride layer.

2.3.1. Conventional Boronizing

The medium for the boronizing process can be either in solid, liquid or gases form. Gas offers a number of distinct technical advantages as a diffusion medium and is used successfully for example nitriding and chromizing. However, due to unsolved problems and serious deficiencies that remain unrectified, gas and liquid phase boronizing have not become state of the art. Technological variants of boronizing process are therefore based solely on solid or powder pack boronizing is used. Yet, it is simple, economical and industrial reliable (Goeuriot *et al.*, 1981).

In the process, the workpiece is placed in a suitable container and embedded in the boronizing agent, which is the activated boron carbide. To avoid oxidation, boronizing should be performed in a protective gas atmosphere, which may be pure nitrogen or a mixture of hydrogen and either argon or nitrogen. In powder pack boronizing, the high cost of boronizing agent and protective environment has severely limited its applications. One way to bring down the cost is by reducing the thickness of the boronizing powder to be packed around the component to the minimum required level without compromising on the properties of the boride layers.

It was found that the boride layer thickness increased with the decrease in carbon content of the material (Meric *et al.*,2000). Furthermore, it was also learnt that the boride layer adhered well to carbon steels and high chromium steels but unsatisfactory results were obtained with very high alloyed steels such as 18-10 stainless steel (Goeuriot *et al*,.1981). The concentration profiles developed during boronizing revealed

different behaviours: carbon segregates towards the matrix, nickel segregates toward the surface, whereas chromium is affected. The segregation of nickel to the surface at high boron activities severely hinders the successful boronizing of highly alloyed steels, e.g. austenitic stainless steels (Goeuriot *et al.,* 1982).

2.3.2. Superplastic Boronizing

Superplastic boronizing (SPB) is a process that combines boronizing with superplastic deformation. The basic principle of superplastic boronizing process is to conduct boronizing while the specimen is undergoing superplastic deformation (Xu *et al.,* 1996). This process provides much faster boronizing rate than that conventional boronizing (CB) process (Xu *et al.,* 1988). It also produces equiaded boride grains instead of acicular grains after conventional boronizing (Xu *et al.,* 1996). The equiaxed boride structure has better mechanical properties than acicular grain (Xu *et al.,* 1997). The microhardness of the boride layer processed by the superplastic boronizing was more uniform than that produced by the conventional boronizing (Xu *et al.,* 2001). Also, reported by (Xu *et al.,* 1996) that superplastic boronizing increased the fracture strength by 8%, toughness by 18%, and bending flexure by 15%, as compared to conventional boronizing.

As compared with conventional boronizing, the borides grain produced by superplastic boronizing is smaller and non-acicular. When there is imperfection developed along or through boride grains, they will meet new grains. Thus, the imperfection has to change their propagation direction which consumes energy and slow down the propagation

speed of the imperfection. All of this factor reduce brittleness and improve the mechanical properties of the boride layers produced by superplastic boronizing.

2.4. Duplex Stainless Steel

Duplex stainless steel (DSS) is defined as a family of stainless steel consisting of a two phase aggregated microstructure of α-ferrite and γ-austenite (Han and Hong, 1999). The balanced 50% α-ferrite and 50% γ-austenite microstructure is obtained by controlled chemical analysis and heat treatment, to produce optimum properties (Charles and Vincent, 1997). Duplex stainless steel itself has the properties of resistance to stress corrosion cracking, high tensile strength, high fatigue strength, good toughness even at low temperature and adequate formability and weldability. These factors promote DSS as suitable alternative to conventional austenite stainless steel. Duplex stainless steels (DSSs) have become established materials, successfully employed in many industrial applications. Their combination of mechanical properties and corrosion resistance is particularly appreciated in the petrochemical field (Cabrera, 2003). DSS has become established materials in many industrial applications such as in oil and gas extraction, paper manufacturing and chemical industries (Cabrera *et al.,* 2003; Charles and Vincent, 1997; Tuomi *et al.,* 2000).

Figure 2.5 shows micrograph of duplex stainless steel and austenitic stainless steel for comparison. The duplex microstructure shows a balance 50% α-ferrite (dark area) and 50% γ-austenite (light area). Figure 2.6 shows a pseudo-binary Fe–Cr–Ni phase diagram. As shown in the diagram, duplex stainless steel solidifies initially as ferrite, then transforms in further cooling to a matrix of ferrite and austenite. They solidify

primarily as ferrous alloys and transform at lower temperatures by a solid state reaction partially to austenite. Precipitation of brittle phases leads to a rapid reduction of the toughness and the forming of low alloyed tertiary austenite makes them prone to corrosion. The corrosion resistant group of ferrous austenitic duplex steels shows a rather complex precipitation and transformation behaviour that affects the mechanical and corrosive properties. Most critical, concerning the change of properties, are the precipitations in the temperature field of 650–950 °C. (Pohl, Storz, & Glogowski, 2007)

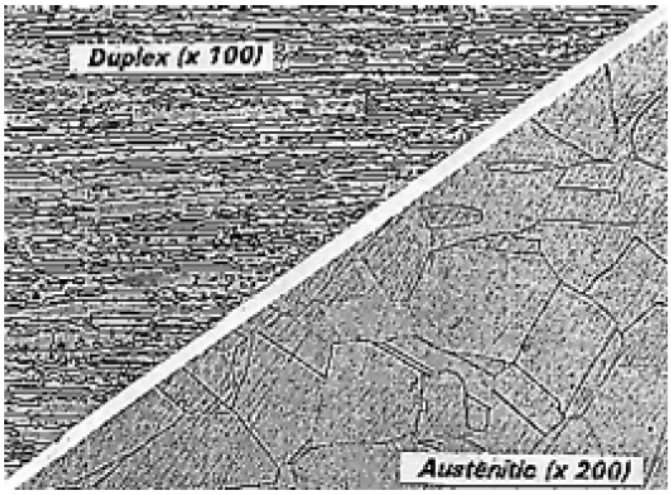

Figure 2.5 Micrograph of both duplex and austenitic stainless steel (Source: Charles and Vincent, 1997)

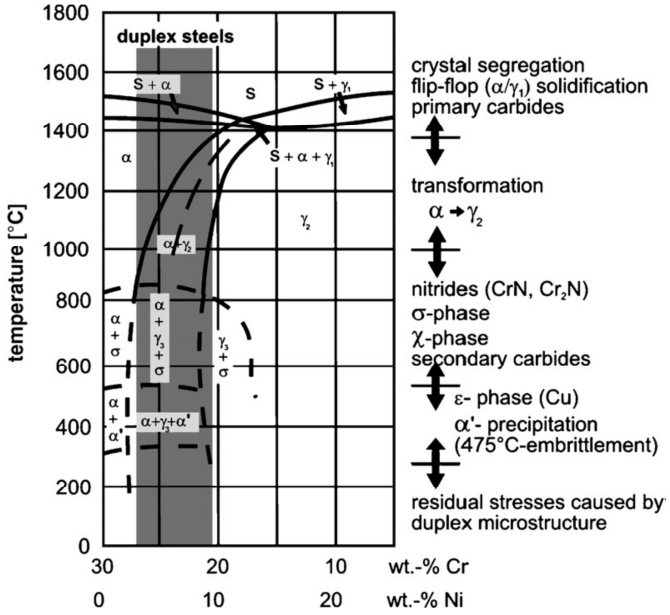

Figure 2.6 Pseudo-binary Fe–Cr–Ni phase diagram (Pohl, Storz, & Glogowski, 2007)

2.5. Superplastic Duplex Stainless Steel

In the last 30 years, duplex stainless steel (DSS) has been studied and characterized as superplastic material. Brief history of superplastic DSS is written paper by Hong and Han (2000) stated that the first reported investigation on the superplasticity in DSS was in 1967 by Hyden *et al.* showed 500% elongation in 25Cr-6.6Ni-0.6Ti hot rolled duplex stainless steel.

Han and Hong (1999) reported that duplex stainless steel with fine grain microstructure has the ability to show superplastic behavior since the grain growth is effectively suppressed at high temperature due to the two phase aggregated microstructure. Since a fine grained microstructure is the most feature of microstructure. Since a fine grained microstructure is the most important feature of superplastic materials, it is known that the processing steps providing the finest microstructures which are stable at the deformation temperature and would enhance superplasticity are definitely important.

Several distinct thermo-mechanical processing technique have been used to develop a superplastic microstructure in duplex stainless steels. One example is thermo-mechanical process consists of hot rolling the material in the temperature range of 1100-1300^{o}C followed by cold rolling with 50% reduction (Jime, 2001). The tensile elongation of superplasticity deformed duplex stainless steel increased with increasing amount of reduction during cold rolling (Han and Hong, 1997). The fine grained duplex microstructure is obtained through the precipitation of the second phase particles when the thermo-mechanically treated duplex stainless steel is heated up at test temperature (Han and Hong, 1999).

It was reported by Jime, (2001) that the mictrostructural evolution during deformation identifies grain boundary sliding as the mechanism responsible for superplastic deformation of duplex stainless steel. On the other hand, some previous studies suggested that the dynamic recrystallization of the softer phase in duplex stainless steel or other duplex microstructure, which occur continuously during deformation could be the dominant mechanism for superplasticity at temperature in the range 800-1100^{o}C. However, Tsuzaki *et al.*,(1996) suggested that grain boundary sliding is dominant mechanism for superplasticity in duplex stainless steel, and that the role of dynamic recrystallization is to keep the grain size fine, suitable for grain boundary sliding. Furthermore, the study connected by Han and Hong (1999) also concluded that the grain boundary sliding assisted by dynamic recrystallization is considered to be the controlling mechanism for superplastic deformation of DSS.

2.6. Tools for processing materials

Tools for processing materials are the key elements in hot and cold forming processes i.e. from the melt (e.g. pressure die casting and powder metallurgy), by hot working (e.g. forging and extrusion) and separation (e.g. shear cutting and chipping). The shape of the tools is preserved by using different hardness that depends on the type of application. In practice, this leads to the following reference values for the service hardness: pure polymer processing 30 – 35 HRC, metal processing 40 – 50 HRC (hot) and 55 – 65 HRC (cold). Greater hardness or hard layers may be required if the wear behaviour is of particular importance. Tools for processing materials are generally made of tool steels, whose properties can be appropriately tailored by the production method, alloying and heat treatment. (Hans & Werner, 2008)

Cutting tool is the tool that used to remove material from the work piece by means of shear deformation. An ideal cutting tool material will combine high hardness with good toughness and chemical stability (Settineri & Faga, 2006). There are several ideal based on the characteristics of the cutter that should be taken into consideration for cutting tool material before it is chosen as one. The characteristics are, the cutting material is harder that the work it is cutting, high temperature stability, resists wear and thermal shock, impact resistant and chemically inert to the work material and cutting fluid. Cutting tools are subjected to high stresses by modern machining technologies, like dry machining, high-speed machining or high-performance machining. The development of new processes demands adapted cutting tools. An ideal cutting material combines high hardness with good toughness and chemical stability (Byrne, Dornfeld, & Denkena, 2003).

Table 2.1 High speed steels (EN ISO 4957): Common high speed steels (HSS) with annealed/service hardnesses and fabrication. (Hans & Werner, 2008)

W-Mo-V-Co	C content	Annealed hardness	Service hardness	Fabrication
[%]	[%]	[HB]	[HRC]	
HS6-5-2	0.87	240 - 300	60 - 64	IM, PM
HS6-5-3	1.2	240 - 300	62 - 65	IM, PM
HS6-5-2-5	0.92	240 - 300	62 - 67	IM
HS10-4-3-10	1.3	240 - 300	60 - 64	IM
HS12-1-4-5	1.4	240 - 300	61 - 65	IM
HS18-1-2-5	0.8	240 - 300	63 - 66	IM
HS2-10-1-8	1.1	240 - 300	67 - 69	IM
HS6-5-4	1.3	< 280	64 - 66	PM
HS4-3-8	2.5	< 300	58 - 66	PM
HS6-7-6-10	2.3	< 340	60 - 69	PM

IM = ingot metallurgy, PM = powder metallurgy

Table 2.1 gives an overview of common high speed steels. The longest service life for continuous cutting is obtained with carbide and cobalt rich steels such as HS10-4-3-10 or HS12-1-4-5. In contrast, for discontinuous cutting applications and higher work piece strength, tougher steels, such as HS6-5-2-5, are more popular. PM steels are suitable for delicate tools, e. g. tap drills, on account of their good toughness. They can also be used as precision cutting punches or cold-heading punches because of their high yield strength.

HSS have a lower wear resistance and hot hardness than hard metals, cutting ceramics, cubic boron nitride (CBN) and polycrystalline diamond (PCD). Nevertheless, their good machinability in the annealed state (hardness 240 - 300 HB), their comparatively good toughness in the hardened and tempered state as well as their less costly manufacturing offer decisive advantages over the above-mentioned cutting materials with a high hard-phase content that can only be produced from powder. High-speed steels protected by

thin films have a comparable or even superior performance to cutting materials containing hard phases. Hard phases deposited by PVD have proven to be effective coatings. (Hans & Werner, 2008)

2.7. Coating Method of Cutting Tool

Owing to the fact that the service life of a tool is determined by the properties of its surface and or near-surface zone, various methods are employed for surface finishing. In addition to surface layer treatments, which have been used for decades, the deposition of thin coatings has become a very popular method in recent years to provide wear protection on tools used for processing materials. Thin (<15µm) layers of hard materials have a high hardness, a high compressive strength, a low adhesion tendency and often low coefficients of friction. They can thus greatly increase the service life of the tool. They are deposited as mono or multilayers from the gas phase either chemically (chemical vapour deposition, CVD) or physically (physical vapour deposition, PVD). (Hans & Werner, 2008)

2.7.1. CVD coatings

The CVD process is based on the reaction of gaseous metal compounds (e. g. fluorides, chlorides and bromides) with reactive gases (e. g. CH_4,CO_2,N_2,H_2) in a closed reactor followed by deposition of the product as a thin hard coating on a steel surface. The reaction temperature in the popular high-temperature CVD process is about 1000℃. The activation energy for this reaction can be introduced by heating the substrate or the reactor wall as well as by plasma ignition, magnetic induction or laser beams. CVD

coatings are uniformly thick and can even be applied to complex geometries without shadowing effects. Not only monolayers, but also multilayer coatings are frequently used. From the broad range of hard coatings, which includes oxides, carbides, nitrides and borides, approx. 6 - 9µm- thick TiC layers on TiN have proven successful on steel tools. TiC is often used as the top layer owing to its high hardness. A number of alternating layers of TiN and TiC produces multilayer coatings with an overall thickness of up to 10 µm. Their good adhesion and high toughness make them suitable for high local loads (e. g. embossing). Good adhesion is obtained by diffusion reactions between the coating and the substrate that may occur at high coating temperatures.

In plasma-assisted CVD processes (PACVD), a pulsed low-pressure glow discharge - with the substrate as the cathode - leads to a higher internal energy in the gas compared to the thermodynamic equilibrium. This allows the process temperature to be lowered to 250 - 600℃ and the tools can be coated after secondary tempering. The process parameters must be carefully selected to match the substrate and the coating materials to achieve good adhesion, particularly at low processing temperatures

PACVD can also be used to deposit superhard boride layers (thickness 1 -3µm): TiN is deposited first as an adhesive base coat, and then the proportion of BCl3 is slowly increased so that the composition gradually changes to TiBN and finally to a top coat of TiB2, which is even harder. Multilayer coatings of TiB, TiN and TiBN are also used (Figure B.5.9 b). Boride coatings have a high thermal stability and their oxidation resistance is only exceeded by that of TiAlN coatings. A combination of plasma nitriding and subsequent PACVD is used to deposit load-bearing layers on substrates with < 60HRC.

Crystalline diamond layers and diamond-like carbon (DLC) layers, which are included, have now become increasingly popular, mainly because of their very low coefficients of friction when paired against various solid materials. They can be deposited by PACVD or PVD as highly cross-linked amorphous carbon layers (a-C films) at 150 - 250℃. The process-related inclusion of hydrogen (10 - 30 atom-%) to produce C:H layers allows the proportion of diamond-like bonds and thus the layer properties (e. g. hardness, adhesion, toughness, coefficients of friction) to be controlled via the processing parameters. Furthermore, DLC layers can be adapted to the respective application within wide limits by doping with non-metals (e. g. oxygen, nitrogen, boron, fluorine) or metals (e. g. a-C:H:Me where Me=W and Ti). They are frequently used as the top layer in mono- and multilayer coatings on account of their low coefficient of friction. (Hans & Werner, 2008)

2.7.2. PVD coatings

The physical deposition of hard coatings from the gas phase involves vaporization of one or more solid sources to form a gas, which may react with a reactive gas (e.g; N_2,CH_4,C_2H_2,CO_2), and then condenses on the substrate as a carbide, nitride or oxide. Of the many different PVD processes known today, cathode sputtering as well as electron beam and arc evaporation have become established processes for producing hard coatings.

This process involves placing tools with a polished and degreased surface in a vacuum chamber that is evacuated and then filled with an inert gas, usually argon, to a pressure of 5Pa. A negative voltage is applied to the substrate connected as the cathode. This

voltage is gradually increased until a self-sustaining glow discharge develops around the substrate that cleans it by ion bombardment (sputter etching). Subsequently, with the glow discharge burning, the source material is vaporized, e.g. by an electron beam, and then condenses on the substrate, whereby the deposition rate must be greater than the sputter rate.

During continuous bombardment, ions are able to penetrate the growing layer thus producing a higher lattice defect density, microstructural refinement, densification of the layer and good adhesion. An arc evaporator (arc PVD) produces a significantly higher ion density than an electron beam evaporator. In this case, the path of the arc is either left un- controlled or it is controlled by an additional magnetic field so that it tracks over one or more arbitrarily located solid source targets that vaporize within the small focal spot.

Cathode sputtering involves the bombardment of Argon ions accelerated against the source material connected as the cathode by ignition of a glow discharge. This ejects particles that are guided by a magnetic field and deposited as a layer on an opposing substrate (magnetron sputtering). Ion bombardment of the substrate can also be increased in this case by glow discharge. Although the adhesion and deposition rate are higher for arc evaporation than for cathode sputtering, they are still significantly lower compared to CVD coating. However, the structure and thickness of the sputtered layer are much more homogeneous compared to arc evaporation. (Hans & Werner, 2008)

CHAPTER 3

3. MATERIALS AND SPECIMEN PREPARATION

3.1.1. Materials

Duplex stainless steel with proportion of 50% α-ferrite and 50% γ-austenite was used as a substrate material in this research. The chemical composition of the material was confirmed by Shimadzu OES-5500II as shown in the table 3.1.

Table 3.1 Chemical composition of duplex stainless steel (JIS SUS329J1) in wt%

C	Si	Mn	P	S	Ni	Cr	Mo	Fe
0.06	0.42	0.30	0.03	0.06	4.18	24.5	0.49	Bal

In order to obtain fine grain microstructure of DSS, the as-received DSS was initially solution treated at 1573 K for one hour, and then followed by water quenching. It was then cold rolled to a plate with 75% of reduction area. Figure 3.1 shows the schematic diagram of thermo-mechanical treatment process.

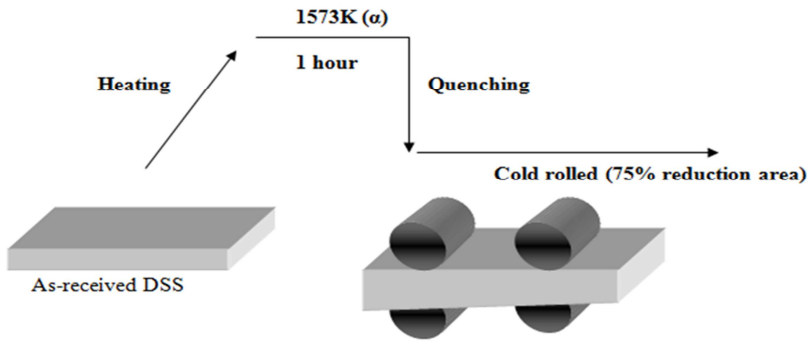

Figure 3.1 Schematic diagram of thermo-mechanical treatment process on DSS

3.1.2. Material Preparation

Sample was cut into a designated dimension of diameter = 7.575 mm, and thickness = 1.7 mm by using wire cutting machine as shown in Figure 3.2. Before conducting boronizing process, the surfaces of the specimen were grounds by using emery paper of grit size 240 to obtain a certain degree of flatness. Then, the specimen were immerse in the alcohol solution to remove grease and any contaminant.

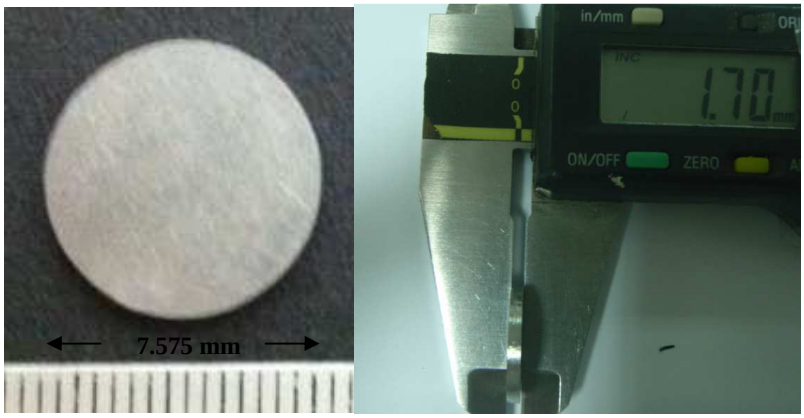

Figure 3.2 Duplex Stainless steel samples

3.2. Die and jigs preparation

Special die and jigs are fabricated for forming of duplex stainless steel sample into designated cutting tool product. The material used for the fabrication of jig and die is stainless steel, where this material is appropriate for hot forming of duplex stainless steel. Furthermore, this material has also undergone boronizing process in order to have sufficient rigidity during forming. Design and the dimension of die and jigs are shown in Figure 3.3.

Properties of materials that determine their selection as die materials for hot forging are: ability to harden uniformly, wear resistance (ability to resist the abrasive action of hot metal during forging), resistance to plastic deformation (ability to withstand pressure and resist deformation under load), toughness, resistance to thermal fatigue and heat checking, and resistance to mechanical fatigue (ASM Handbook Vol 14, Forming and Forging, S.L. Semiatin et al., 1998). The material used in fabrication of die set was Chromium-based AISI hot work tool steels H 13.

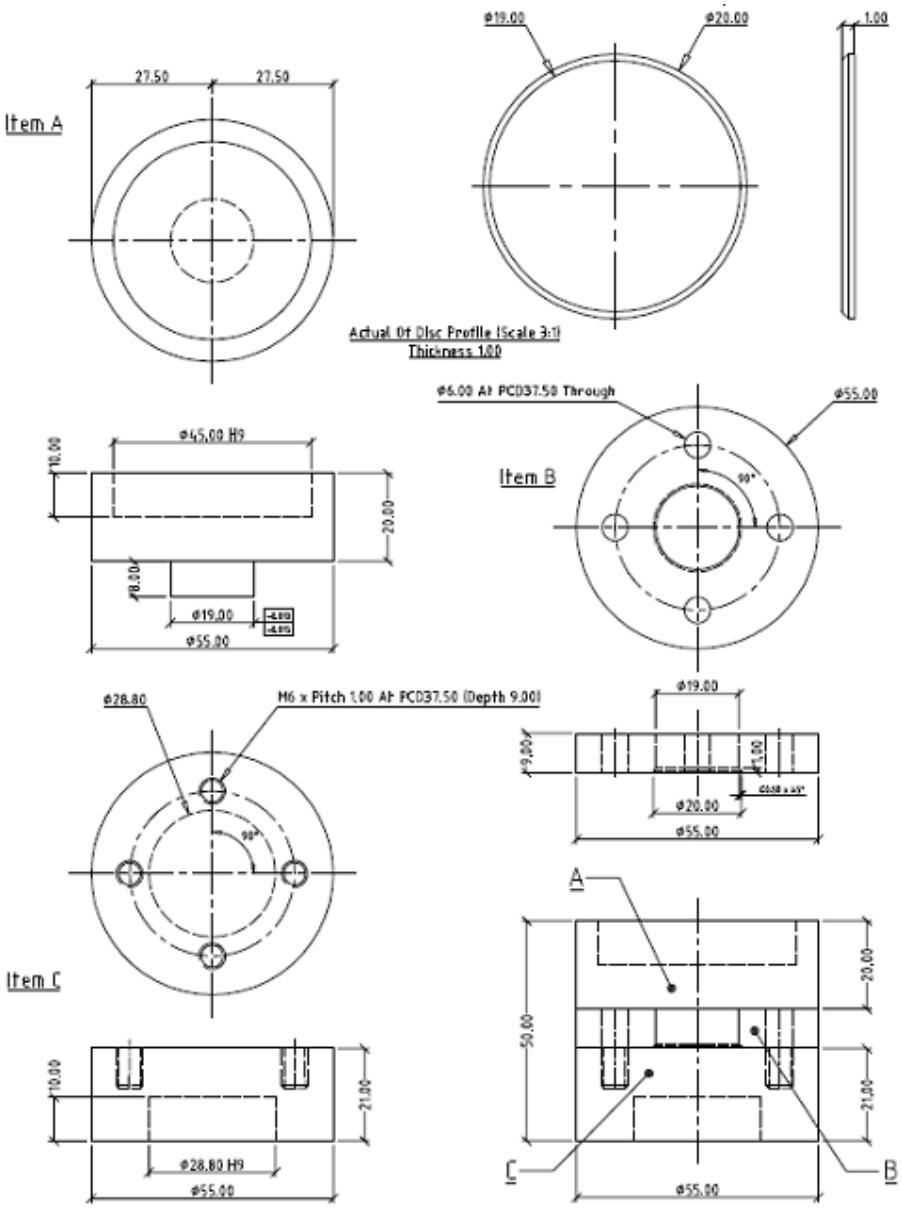

Figure 3.3 Dimension of die

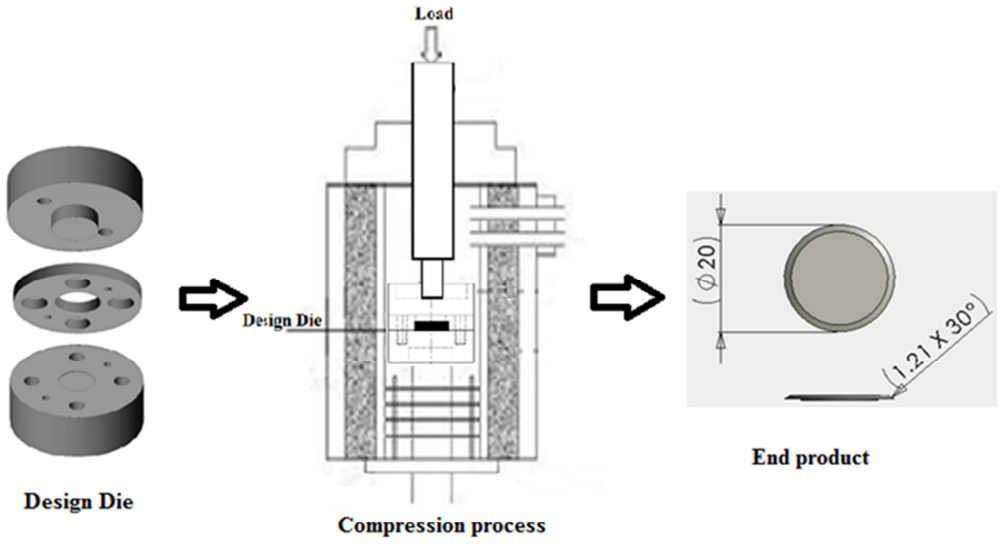

Figure 3.4 Flow diagram of the experimental work

3.3. Boronizing Procedure

3.3.1. Conventional Boronizing Procedure

For conventional boronizing, the specimen was placed inside the cylindrical container. The specimen was packed in the middle of the container surrounded with boronizing powder. After boronizing powder was fully filled in the container, the container was tapped until the powder was fully packed. Figure 3.5 and 3.6 shows container used for conventional boronizing process.

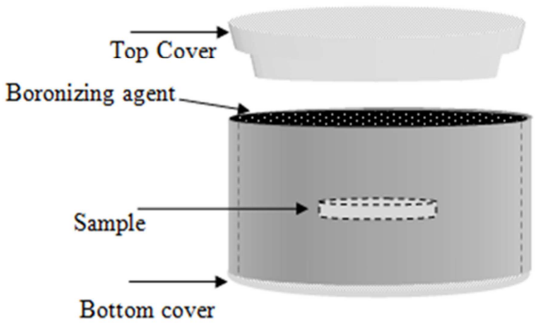

Figure 3.5 Schematic diagram of the stainless steel cylindrical container

Figure 3.6 Cylindrical container use in conventional boronizing

The conventional boronizing process is performed at 1223K in a tube furnace with controlled atmospheric condition using argon gas as shown in Figure 3.7. The argon gas was constantly supplied until the end of the process. In order to have a conservative hardness value, boronizing time is kept for 6 hours. After the boronizing process finished, the specimen was kept in the furnace for cooling down to room temperature.

Figure 3.7 Tube Furnace (Carbolite, type CTF 17/75/300, Max temp: 1973 K)

For all sample, Ekabor-1 powder was used as the boronizing agent with powder grain size of 150µm during boronizing process. This method, in which the boronizing agent is in powder form, has a wide range of applications because of its many advantages, including ease of treatment, ability to achieve a smooth surface, and simplicity of the required equipment (Meric, 2000). The boronizing agent is placed into the heat-resistant box, and specimens are embedded into this powder. A large contact surface is desired between the material and boronizing agent, to allow better diffusion of boron atoms into the material surface. The particle size of the powder is an important factor in the formation of the boride layer. (Meric, 2000)

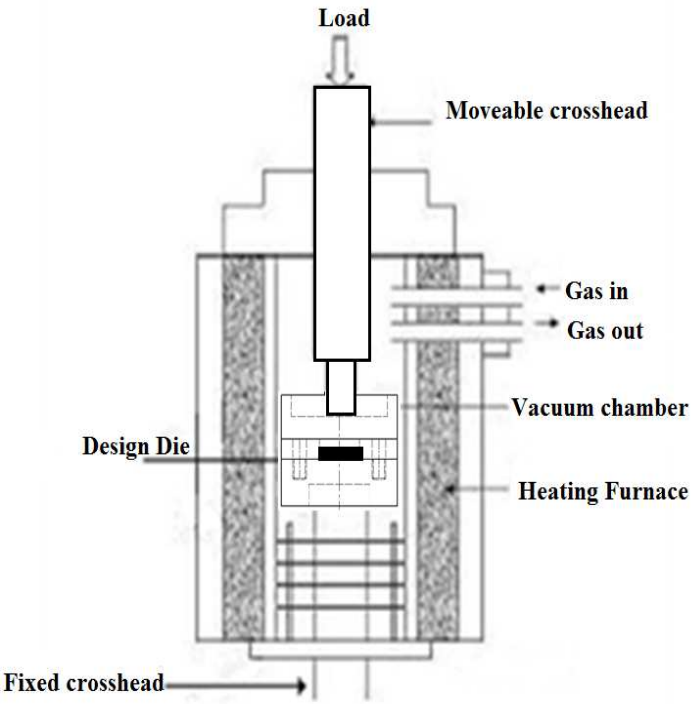

Figure 3.8 Schematic diagrams of the experimental forming apparatus

3.4. Superplastic deformation

The compression process is conducted using a compression test machine (Instron) equipped with a high-temperature furnace in Argon gas atmosphere which is shown in Figure 3.9. This process must be done under a controlled gas atmosphere in order to avoid diffusion of oxygen, nitrogen and hydrogen gasses into the duplex stainless steel which will cause the duplex to become more brittle. Substrates are heated from room temperature to 1223 K and then it is maintained at this temperature for 5 minutes to ensure thermal equilibrium. Then the substrate is pressed by movable crosshead to the reduced height at a specified strain rate and strain. Figure 3.10 shows the schematic diagram of compression test process involved.

Figure 3.9 Instron machine used for the superplastic deformation process

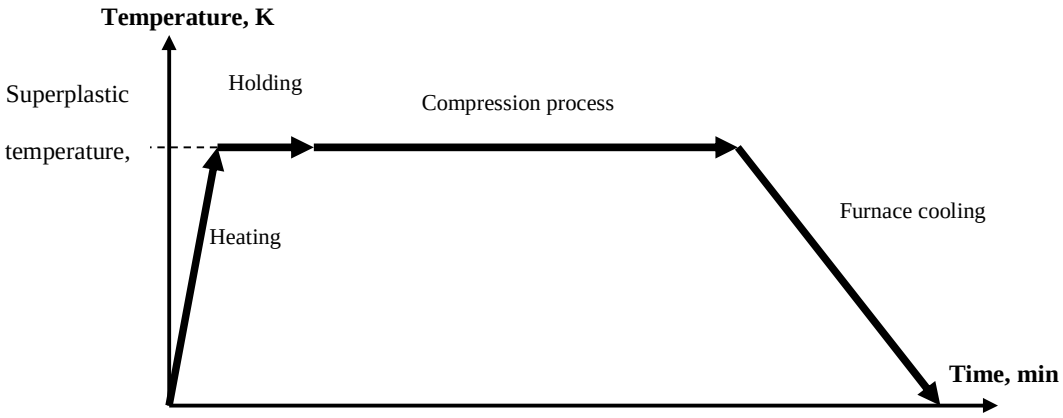

Figure 3.10 Compression process flow diagram

3.5. Grinding and Polishing

Grinding is the most important operation in specimen preparation in order to eliminate the effects of sectioning. All of the specimens are ground on successively fine grades of emery paper to remove any irregularities and oxide layer prior to embedment process. The grades (mesh size no.) of emery paper used are 100 and 200. The grid paper starting with the coarsest, 100 to 200 is laid on centrifugal grinder as shown in Figure 3.11 and the surface to be embedded is held face downwards until a flat and smooth surface with parallel lines is produced. After the grinding process, specimens are pickled with alcohol to remove contaminants.

Prior to microstructure evaluation, polishing is done on embedded samples in order to remove scratches and deformation from grinding and achieve a surface that is highly reflective, flat and defect free. The polishing machine used is shown in Figure 3.12. Samples are polished until a mirror like surface is obtained. For microstructure study, special etchant for duplex stainless steel was prepared from hydrochloric acid (HCl) saturated with ferric chloride (FeCl3) and activated with small amount of nitric acid (HNO3) by following the proportion as mention by Voort (1984) in his Metallography book. The purpose of etching is to optically enhance microstructural features such as grain size and phase features (Internet source-1).

Figure 3.11 Rotary pre-grinder

Figure 3.12 Polishing machine

3.6. Characterization methods

Several characterization techniques were used to study the macro and micro of the boronized specimen. X-ray diffraction analysis was conducted to confirm the presence of boride phase on the boronized layer. The microstructure of the specimen was studied using the optical microscope and scanning electron microscope (SEM). The surface hardness was also measured before and after boronizing process.

3.6.1. X-ray Diffraction

X-ray diffraction (XRD) is one of the most powerful techniques for qualitative and quantitative analysis of crystalline compounds. The wavelengths of X-rays are of the same order of magnitude as the distances between atoms or ions in a molecule or crystal (Å, 10^{-10} m). A crystal diffracts an X-ray beam passing through it to produce beams at specific angles depending on the X-ray wavelength, the crystal orientation, and the structure of the crystal. X-rays are predominantly diffracted by electron density and analysis of the diffraction angles produces an electron density map of the crystal (Internet source-2). XRD is a nondestructive technique that provides detailed information about the chemical composition and crystallographic structure of natural and manufactured materials. X-ray diffraction (XRD) spectra of the specimens before and after boronizing were determined using Philips X'Pert MPD PW3040 XRD with CuKα radiation at 1.54056 Å X-ray wavelength. The specimen were scanned from 10^{o} to 80^{o} 2Θ angle at step sice of 0.020 and a count time of 1.5 s at each step (Ismail, 2004)

Figure 3.13 XRD Machine (Internet source-3)

3.6.2. Scanning electron microscope

The scanning electron microscope (SEM) is a type of electron microscope that creates various images by focusing a high energy beam of electrons onto the surface of a sample and detecting signals from the interaction of the incident electrons with the sample's surface. The electrons interact with the atoms that make up the sample producing signals that contain information about the sample's surface topography, composition and other properties such as electrical conductivity.

The SEM has many advantages over traditional microscopes. The SEM has a large depth of field, which allows more of a specimen to be in focus at one time. The SEM also has much higher resolution, so closely spaced specimens can be magnified at much

higher levels. Since the SEM uses electromagnets rather than lenses, the degree of magnification can be control. All of these advantages, as well as the actual strikingly clear images, make the SEM one of the most useful instruments in research today.A Jeol JSM6310 SEM operating with an accelerating voltage of 25 kV was used to examine the microstructure of the materials (Figure 3.14).

Figure 3.14 Scanning electron microscope (SEM)

3.6.3. Energy Dispersive X-ray Analysis

Energy dispersive X-ray spectroscopy (EDX) is an analytical technique used for the elemental analysis or chemical characterization of a sample. As a type of spectroscopy, it relies on the investigation of a sample through interactions between electromagnetic radiation and matter, analyzing x-rays emitted by the matter in response to being hit with charged particles. Its characterization capabilities are due in large part to the fundamental principle that each element has a unique atomic structure allowing x-rays that are characteristic of an element's atomic structure to be identified uniquely from each other.

EDX systems are most commonly found on SEM-EDX and electron microprobes. SEM is equipped with a cathode and magnetic lenses to create and focus a beam of electrons and have been equipped with elemental analysis capabilities.

Figure 3.15 SEM-EDX OXFORD Instrument, INCA Energy 400

3.6.4. Microhardness Test

Hardness is the property of a material that enables it to resist plastic deformation, usually by penetration. The greater the hardness of the metal, the greater resistance it has to deformation. The term of hardness may also refer to resistance to bending, scratching, abrasion or cutting (Internet source-4).

The Vickers hardness test is a method of determining the hardness of materials whereby a diamond pyramid is pressed into the surface of the specimen and the diagonals of the

impression are measured with a microscope fitted with a micrometer eye piece. The rate of application and duration are automatically controlled and the load can be varied (Internet source-5). The advantages of the Vickers hardness test are that extremely accurate readings can be taken and just one type of indenter is used for all types of metals and surface treatments.

The microhardness test method according to ASTM E-384 specifies a range of loads using a diamond indenter to make an indentation, which is measured and converted to a hardness value. In this research, the hardness of embedded surface is measured using a Mitutoyo MK-17 series microhardness tester with an applied load of 2N and loading time of 10s (Figure 3.16).

Figure 3.16 Vickers microhardness tester

3.6.5. Optical Microscope

The optical microscope, often referred to as the "light microscope", is a type of microscope which uses visible light and a system of lenses to magnify images of small samples. Basic optical microscopes can be very simple, although there are many complex designs which aim to improve resolution and sample contrast. Historically optical microscopes were easy to develop and are popular because they use visible light so that samples may be directly observed by eye. (Internet reference – 6)

The optical microscope is used in microstructural analysis and determination of boronized layer thickness and morphology. The optical microscope Zeiss Aziotech with maximum 1000 times enlargement was connected by a Panasonic camera model WV-CP410 to an image analyzer MSQ software version 6.5. The digital camera captures and displays the image from the optical microscope directly to the computer screen.

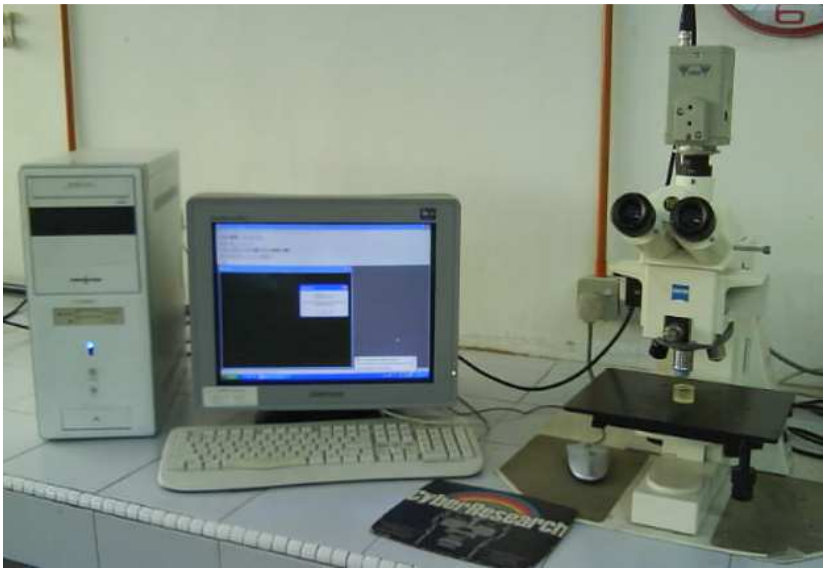

Figure 3.17 Optical microscope with image analyzer system

CHAPTER 4

4. RESULTS AND DISCUSSIONS

4.1. Substrate Material

In this study a thermo-mechanically treated DSS with fine microstructure was used. The optical microstructure of thermo-mechanically treated after heated at boronizing temperature is shown in figure 4.1. The hardness of the fine grain is ± 420 HV. DSS with fine grain microstructure has the ability to show superplastic behavior at high temperature.

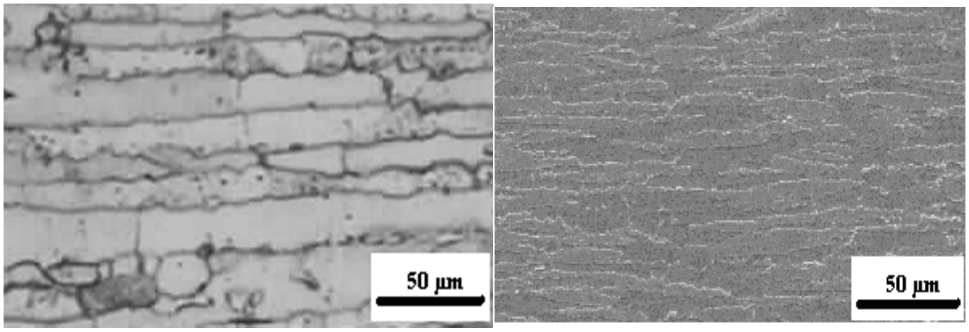

(a) (b)

Figure 4.1 (a) Optical image of as-received DSS (b) SEM image of as-received DSS

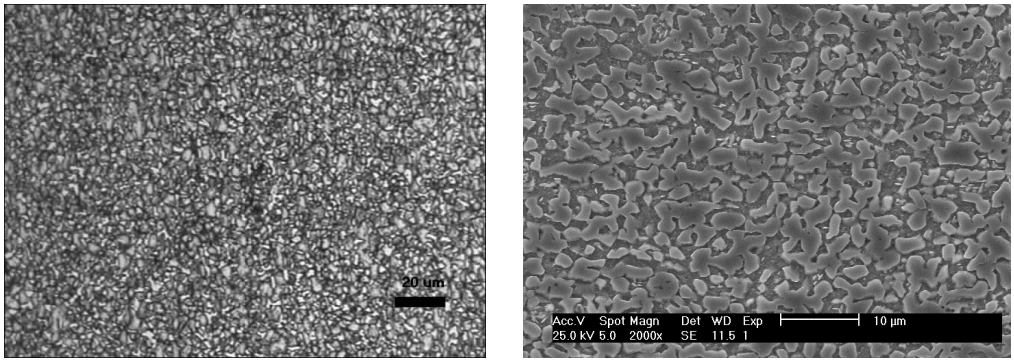

(a) (b)

Figure 4.2 (a) Optical image of fine microstructure DSS (b) SEM image of fine microstructure DSS

4.1.1. Boride Phase - X-ray Diffraction Analysis

The presence of boride phases on the boronized specimens was confirmed by X-ray diffraction (XRD) analysis. Figure 6 shows the typical XRD pattern of the DSS before and after boronized. From the relative peak intensity in the XRD pattern, the presence of boride phases of FeB, Fe_2B and CrB are detected on the DSS, proving that boronizing was successful.

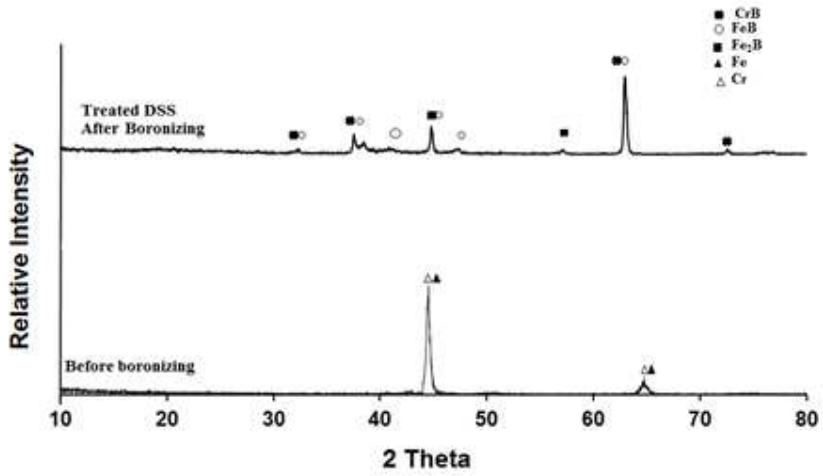

Figure 4.3 X-ray diffraction pattern of superplasticity boronized DSS

4.1.2. Boronized layer thickness

Layer thickness on boronized specimens prepared for metallographical investigation using optical microscope. Figure 4.3 shows a SEM cross-sectional view of superplastically boronized DSS at 1223 K for 6 hours. The uniformity of boride layer can clearly distinguished as a darker area and brighter area of diffusion zone and the DSS substrate. The morphology of boride layers was found uniform, compact and

smooth. It was reported by (Özbek, Konduk, Bindal, & Ucisik, 2002) that the compact and smooth morphology is due to high alloying elements in stainless steel.

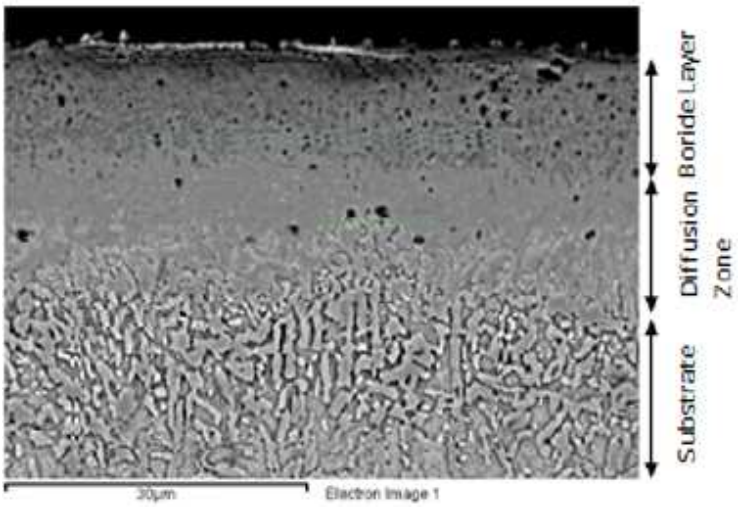

Figure 4.4 SEM cross-sectional view of DSS

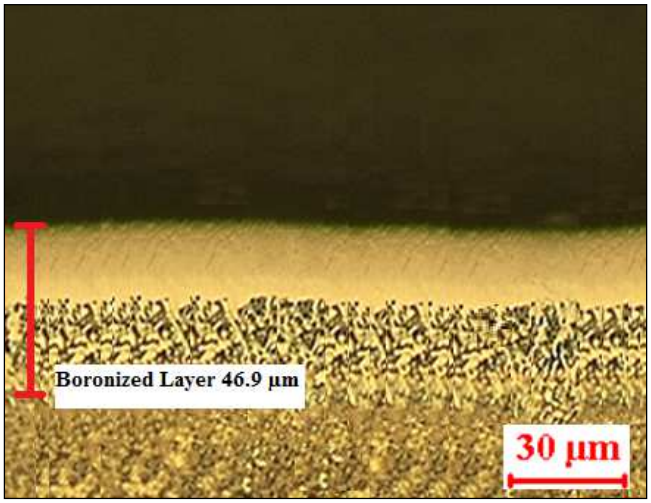

Figure 4.5 View of boride layer after boronizing at 1223 K for 6 hours

The thickness of boride layer ranged from 39 µm to 46.9 µm respectively. The boronizing process parameter used in this study is assumed as an optimum parameter derived from other studies.

4.1.3. Hardness Profile

Micro hardness measurements were performed from the surface to interior along a line to check variation of hardness in the boronized layer as in figure 4.5. The results show the gradual decrease in hardness from the surface region to the core.

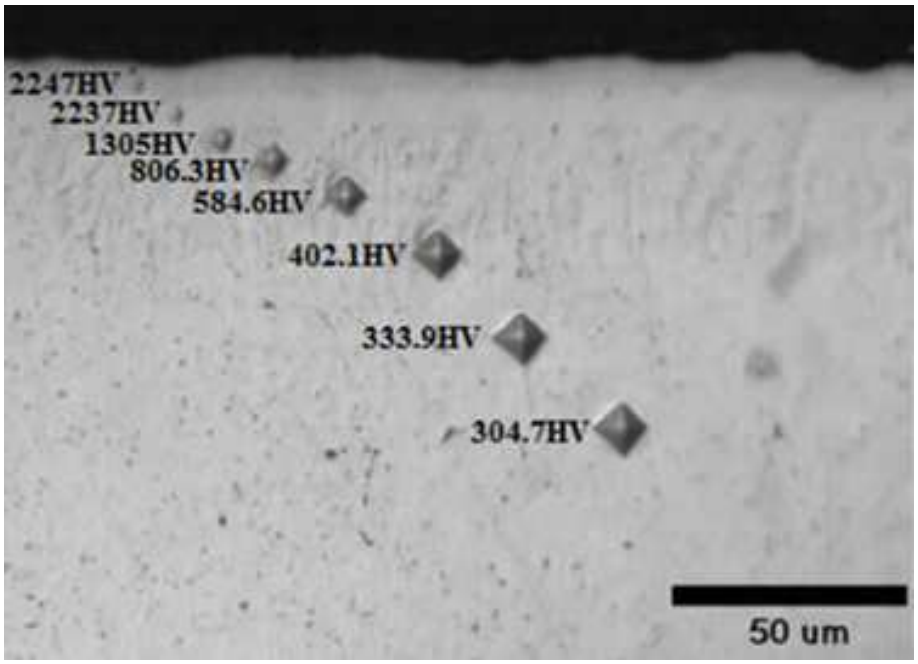

Figure 4.6 Optical micrographs showing variation indentation hardness

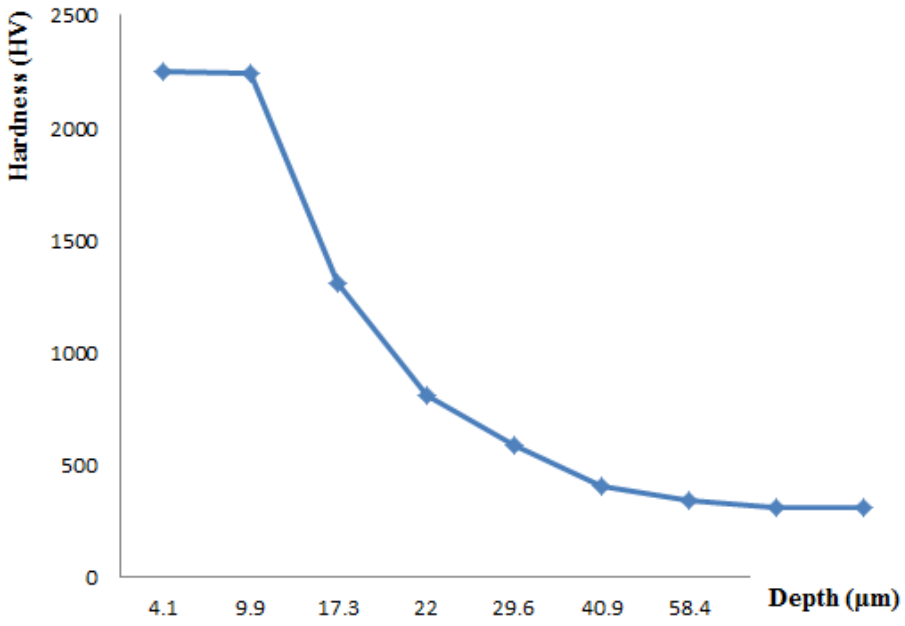

Figure 4.7 Cross section hardness profile of boronized fine microstructure DSS as a function of depth.

It can be seen in figure 4.6 that the hardness of boride layer is considerably higher than that of the steel matrix.

4.2. Forming Process

Figure 4.7 shows plane and cross section view of the representative sample taken before and after forming process. It is apparent in the photograph that the specimen has great compressibility and can be perfectly deformed without macro surface disintegration. At the same time, the actual elastic strain has also been absorbed by the die which had simultaneously deformed. The selection of die material may need further evaluation in the future development.

Figure 4.8 View of cutting tool specimen before and after deformation

Table 4.1 Summary of specimen measurement before and after deformation

Specimen	Strain Rate	Strain	Thickness Before	Thickness After	Diameter Before	Diameter After
A	$1x10^{-4}$	0.8	1.7 mm	1.6 mm	15 mm	15.7 mm
B	$9x10^{-5}$	0.4	1.7 mm	1.65 mm	15 mm	16.3 mm
C	$9x10^{-5}$	1.0	1.7 mm	1.5 mm	15 mm	17.6 mm

It can be seen that the higher strain applied will caused more reduction in thickness of the specimen as presented in the above Table 4.1. It is apparent that sample C has shown excellent compressibility and can be perfectly deformed without macro surface disintegration. Die material was observed to have deformation after several compressions under the influence of high temperature.

4.2.1. Superplastic Flow

The stress-strain curve of the compressed specimen at different strain rate is shown in Figure 4.8. All of the curves exhibit typical continuous dynamic recrystallization (DRX) characteristic where stress increases to peak followed by softening, and then remain constant (Seshacharyulu, Medeiros, Frazier, & Prasad, 2000). The DRX characteristic of the stress is caused by microstructural evolution of work hardening, DRX occurrence and steady state.

The lowest flow stress which is approximately 40 MPa was obtained at the slowest strain rate. The degree of DRX increases with the decrease of strain rate. This is because of DRX (involving nucleation and grain growth) needs time. When stain rate is relatively low, DRX grains have more time to nucleate and grow. At high strain rates, the accumulated energy increases, as dislocations have not enough time to consume or continually generate. The presence of excess dislocation can lead to heterogeneous nucleation of DRX grains. However, the diffusion cannot proceed completely and DRX grain growth is not so pronounced because of the very short deformation time. In accordance with the microstructural evolution, the flow stress increases with the increase of strain rate. Thus, it can be concluded that the lower the deformation strain rate, the easier the process of DRX for the alloy when other condition remain constant.

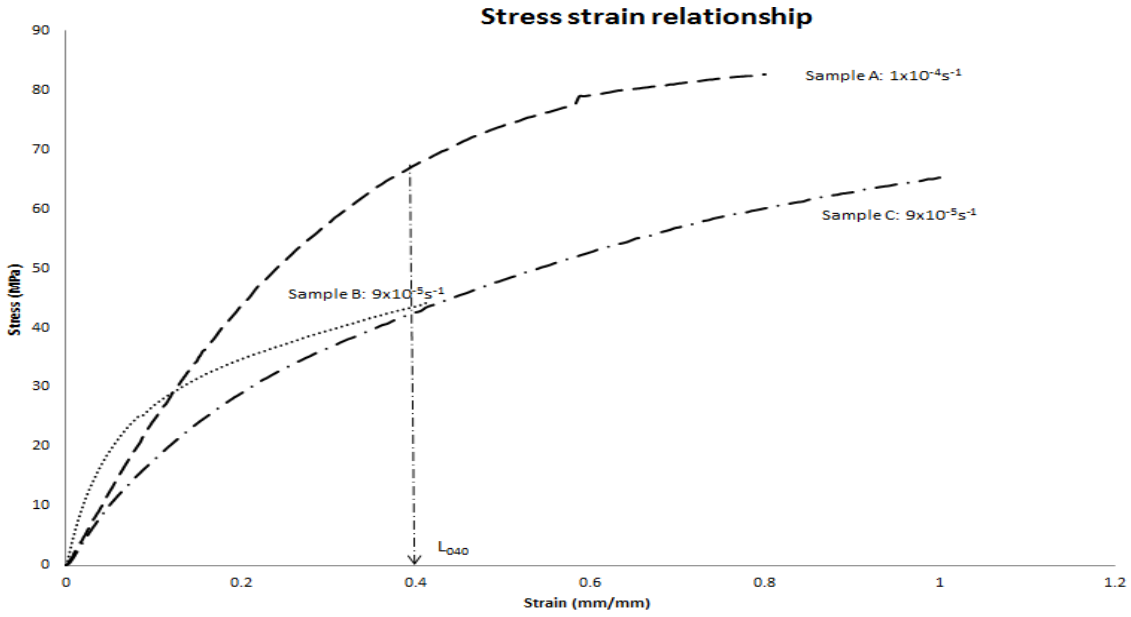

Figure 4.9 Stress and strain relationship at different strain rate and different reduction rate

Figure 4.8 shows the flow stress of the sample deformation at different stain rate. At strain of 0.4 (L_{040}), flow stress of sample B and C are lower than A. This comparison shows that the flow stress produced increased when the strain rate is increased. The flow stress is restricted by the movement of the substrate atom and boron layer in a shorter time. Comparison between B and C demonstrate the effect of different stain. It shows that flow stress is almost similar for both sample even strain applied to sample C is higher. It is very important to understand the behaviour of the flow stress and very crucial to maintain the flow stress at lower level to avoid surface disintegration.

4.2.2. Near Surface Microstructure Evaluation

Figure 4.9 depicted the near surface microstructure after forming. From the figure it is obvious that sample B shows the highest quality of near surface condition where no sign of flaws are observed. A sign of flaw in the form of crack is observed in sample A, while in sample C the flaws have deteriorated further results in a phenomenon described here as surface disintegration. As mention in the earlier section, higher flow stress and strain are the reason for these results. From the observation, there is an optimum condition of the stress and strain to avoid surface disintegration. The strain rate and the amount of strain applied are crucial and critical to ensure surface integrity as well as perfectness of the finished product.

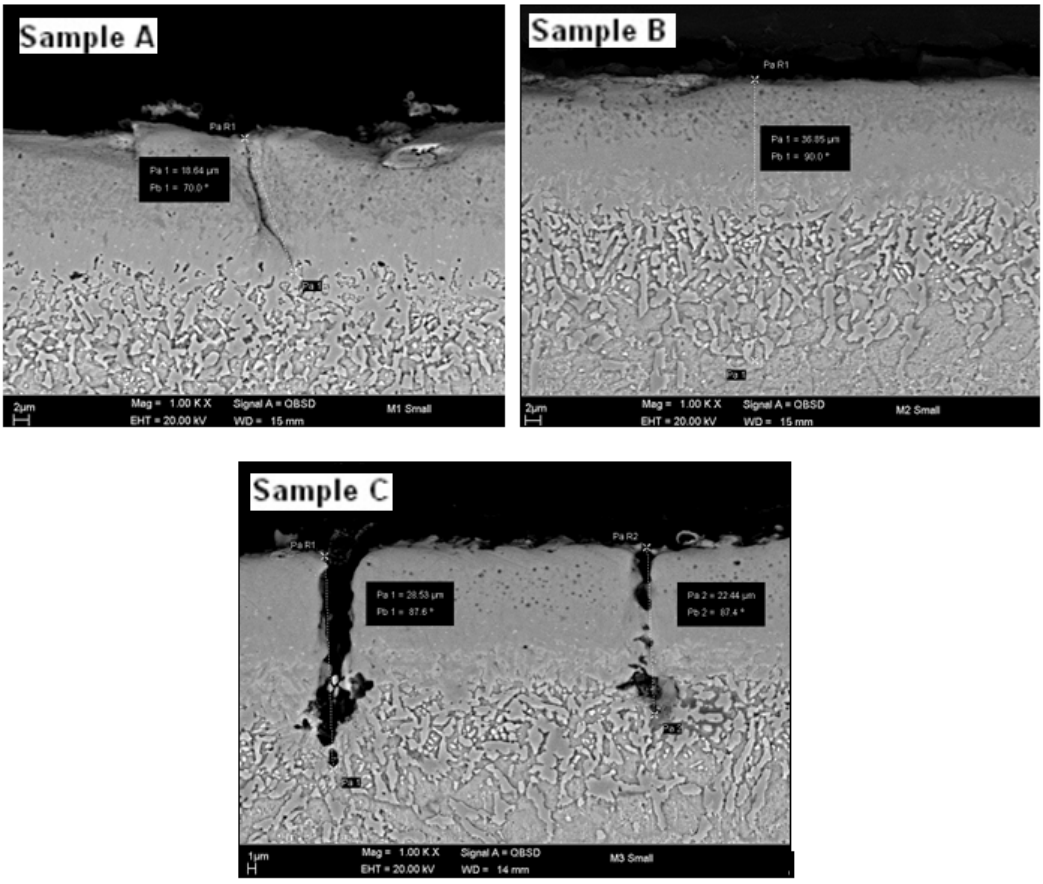

Figure 4.10 SEM images of deformed sample at different strain rate; Sample A; Strain rate = 1 x 10-4 s^{-1} and strain 0.8 mm/mm, Sample B; Strain rate = 9×10-4 s^{-1} and strain 0.4 mm/mm and Sample C; Strain rate = 9×10-4 s^{-1} and strain 1.0 mm/mm

CHAPTER 5

5. CONCLUSIONS AND RECOMMENDATIONS

5.1. Conclusions

In this research, a new method to develop cutting tool from boronized duplex stainless steel through superplastic method is studied. The results are summarized as follows:

(1) Boronizing has successfully performed onto the duplex stainless steel (DSS). It is found evident that the boronized layer shows a smooth and compact morphology with uniform thickness of boronized layer ranging from 39 to 46.3 μm before forming and after hot forming. The cutting tool surface hardness is homogeneous after forming with hardness ranging from 2232HV to 2345HV

(2) Surface integrity was found on the boronized layer which deformed at strain rate of $9x10^{-5}$ s^{-1} and 0.4 mm/mm strain. However, with the same strain rate the sample had failed at 1.0 mm/mm strain due to high strain factor. Surface disintegration also was observed at 0.8 mm/mm strain with $1x10^{-4}$ strain rate due to higher flow stress applied and specimen could not sustain the applied load.

(3) Sample B shows the highest quality of near surface condition where no sign of flaws are observed. A sign of flaw in the form of crack is observed in sample A, while in sample C the flaws have deteriorated further results in a phenomenon described here as surface disintegration. As mention in the earlier section, higher flow stress and strain are the reason for these results.

5.2. Recommendations

Throughout this study, the following consideration can be suggested to improve the implemented method:

(1) To re-evaluate selection materials of cutting tool die and consider an alternative for a new type of material. In the current study, H13 material was observed to have deformed after several compressions under the influence of high temperature. Material such as inconel may be used since inconel possess the ability to retain strength over a wide temperature range and appropriate for high temperature applications.

(2) Further study on deformed cutting tool would be to evaluate the product performance including wear test, chip formation evaluation and corrosion test.

(3) Further study to refine the result on the optimum strain and strain rate parameter as the specific design will have their individual optimum condition.

CHAPTER 6

6. REFERENCES

Ahamad, N. W., & Jauhari, I. (2012). Carburizing of Duplex Stainless Steel (DSS) Under Compression Superplastic Deformation. *Metallurgical and Materials Transactions A*. doi:10.1007/s11661-012-1357-4

Azuar, S., Azis, A., Jauhari, I., Rozlin, N., Masdek, N., Wahida, N., & Hiroyuki, O. (2010). Surface Roughness and Initial Pressure Effect on Superplastically Carburized Duplex Stainless Steel, *301*, 227–232. doi:10.4028/www.scientific.net/DDF.297-301.227

Barnes, a. J. (2007). Superplastic Forming 40 Years and Still Growing. *Journal of Materials Engineering and Performance*, *16*(4), 440–454. doi:10.1007/s11665-007-9076-5

Braham-Bouchnak, T., Germain, G., Robert, P., & Lebrun, J. L. (2010). High pressure water jet assisted machining of duplex steel: machinability and tool life. *International Journal of Material Forming*, *3*(S1), 507–510. doi:10.1007/s12289-010-0818-9

Byrne, G., Dornfeld, D., & Denkena, B. (2003). Advancing Cutting Technology. *CIRP Annals - Manufacturing Technology*, *52*(2), 483–507. doi:10.1016/S0007-8506(07)60200-5

Cabrera, J. M., Ponce, J., & Prado, J. M. (2003). Modeling thermomechanical processing of austenite. *Journal of Materials Processing Technology*, *143-144*, 403–409. doi:10.1016/S0924-0136(03)00441-2

Cabrera, J. M., Ponce, J., & Prado, J. M. (2003). Modeling thermomechanical processing of austenite. *Journal of Materials Processing Technology, 143-144*, 403–409. doi:10.1016/S0924-0136(03)00441-2

Cabrera, J.M., Mateo, A., Llanes, L., Prado, J.M., Anglada, M. (2003). Hot deformation of duplex stainless steels. *Journal of Materials Processing Technology. 143-144.* 321-325

Charles, J. and Vincent, B. (1997). Duplex stainless steels for chemical tankers. *Proceedings of Duplex Stainless Steels 97 - 5th World Conference.* Netherlands. 727-736. Retrived from http://www.stainless-steel-world.net/pdf/d97_018.pdf

Chandra, N. (2002). Constitutive behavior of superplastic materials. *International Journal of Non-Linear Mechanics.* 37. 461-484

Coiley, J.A. (1974). Technology of superplasticity. *Physics in Technology. 5.*86-90. doi:10.1088/0305-4624/5/2/I01

Courtney, T.H., (2000). *Mechanical Behaviour of Materials, 2nd Edition,* McGraw Hill.

Da Costa, C. E., Zapata, W. C., & Parucker, M. L. (2003). Characterization of casting iron powder from recycled swarf. *Journal of Materials Processing Technology, 143-144*, 138–143. doi:10.1016/S0924-0136(03)00394-7

Demaid, A., (1992). A history of superplastic metals [in:] J.H.W. de Wit, A. Demaid, M. Onillon, Case studies in manufacturing with advanced materials - Vol. 1, North-Holland, Amsterdam, 35-71.

Genel, K., Ozbek, I., & Bindal, C. (2003). Kinetics of boriding of AISI W1 steel. *Materials Science and Engineering: A, 347*(1-2), 311–314. doi:10.1016/S0921-5093(02)00607-X

Goeuriot, P., Thevenot, F. & Driver, J.H. (1981). Surface treatement of steels: Borudif, a new boriding process. *Thin Solid Films, 78*(1), 67-76

Han, Y. S., & Hong, S. H. (1997). The effects of thermocmechanical treatments on superplasticity of Fe-24Cr-7Ni-3Mo-0 . 14N duplex stainless steel. *Scripta Materialia, 36*(5), 557–563.

Hans, B., & Werner, T. (2008). *Ferrous materials: steel & cast iron.* Germany: Springer.

Hasan, R., Jauhari, I., Ogiyama, H., & Dadan, R. (2006). Compression Method for Superplastic Boronizing of DSS, *328*, 1745–1748. doi:10.4028/www.scientific.net/KEM.326-328.1745

Hertzberg, R.W., (1937). *Deformation and Fracture Mechanics of Engineering Materials. 4'th ed.* USA: John Willey & Sons, Inc.

Hong, S. H., & Han, Y. S. (2000). Phenomena and mechanism on superplasticity of duplex stainless steels. *Metals and Materials, 6*(2), 161–167. doi:10.1007/BF03026361

Ismail, R. (2004). Fabrication and Properties of Nickel Aluminde-Alumina Intermetallic Composites. M.Eng.Sci Research Dissertation. University of Malaya, Kuala Lumpur, Malaysia. p23

Jain, V., & Sundararajan, G. (2002). Influence of the pack thickness of the boronizing mixture on the boriding of steel. *Surface and Coatings Technology*, *149*(1), 21–26.

Jime, J. A. (2001). Superplastic properties of a d / g stainless steel, *307*, 134–142.

Jauhari, I., Yusof, H. a. M., & Saidan, R. (2011). Superplastic boronizing of duplex stainless steel under dual compression method. *Materials Science and Engineering: A*, *528*(28), 8106–8110. doi:10.1016/j.msea.2011.07.054

Kaibyshev, O.A., (2002). Fundamental aspects of superplastic deformation, Materials Science Engineering A 324, 96-102.

Keddam, M., & Chentouf, S. M. (2005). A diffusion model for describing the bilayer growth (FeB/Fe2B) during the iron powder-pack boriding. *Applied Surface Science*, *252*(2), 393–399. doi:10.1016/j.apsusc.2005.01.016

Keunecke, M., Bewilogua, K., Wiemann, E., Weigel, K., Wittorf, R., & Thomsen, H. (2006). Boron containing combination tool coatings—characterization and application tests. *Thin Solid Films*, *494*(1-2), 58–62. doi:10.1016/j.tsf.2005.08.204

Keunecke, M., Wiemann, E., Weigel, K., Park, S. T., & Bewilogua, K. (2006). Thick c-BN coatings – Preparation, properties and application tests. *Thin Solid Films*, *515*(3), 967–972. doi:10.1016/j.tsf.2006.07.057

Leyens, C., & Peters, M. (2003). *Titanium and titanium alloys: Fundamentals and applications.* Germany: Wiley.

Langdon, T. G., (2009). Seventy-five years of superplasticity: historic developments and new opportunities J Mater Sci 44, 5998–6010.

Mabuchi, M., & Higashi, K. (1998). The Processing , Properties , and Applications of High-Strain-Rate Superplastic Materials, (June).

Maehara, Y., & Ohmori, Y. (1987). Microstructural change during superplastic deformation of δ-ferrite/austenite duplex stainless steel. *Metallurgical Transactions A*, *18*(5), 663–672. doi:10.1007/BF02649482

Martin, R., and Evans, D., (2000). Reducing costs in aircraft: The metals affordability initiative consortium, Journal of The Minerals, Metals & Materials Society 52/3, 24-28.

Matsushita, M., & Ogiyama, H. (2009). Diffusion of Boron on Superplastic Duplex Stainless Steel. *Journal of Phase Equilibria and Diffusion*, *31*(1), 2–5. doi:10.1007/s11669-009-9611-1

Matsushita, M., Suko, T., Matsuda, S., Ohfuji, H., & Ogiyama, H. (2009). Analysis of the texture of superplastic carburized duplex stainless alloy. *Materials Chemistry and Physics*, *114*(2-3), 522–524. doi:10.1016/j.matchemphys.2008.11.051

Meric, C. (2000). Investigation of the effect on boride layer of powder particle size used in boronizing with solid boron-yielding substances, *35*, 2165–2172.

Nakahigashi, J., & Yoshimura, H. (2002). Ultra-fine grain refinement and tensile properties of titanium alloys obtained through protium treatment. *Journal of Alloys and Compounds*, *330-332*, 384–388. doi:10.1016/S0925-8388(01)01528-6

Nieh, T.G., Wadsworth, J., Sherby, O.D., (1997). *Superplasticity in Metals and Ceramics*, Cambridge University Press, Cambridge.

Patankar, S. N., Lim, C. T., & Tan, M. J. (2000). Superplastic forming of duplex stainless steel. *Metallurgical and Materials Transactions A, 31*(9), 2394–2396. doi:10.1007/s11661-000-0158-3

Podgornik, B., Hogmark, S., Sandberg, O., & Leskovsek, V. (2003). Wear resistance and anti-sticking properties of duplex treated forming tool steel. *Wear, 254*(11), 1113–1121. doi:10.1016/S0043-1648(03)00322-3

Ramdan, R. D., Jauhari, I., Hasan, R., & Masdek, N. R. N. (2008). The role of strain rate during deposition of CAP on Ti6Al4V by superplastic deformation-like method using high-temperature compression test machine. *Materials Science and Engineering: A, 477*(1-2), 300–305. doi:10.1016/j.msea.2007.05.038

Sagradi, M., Pulino-Sagradi, D., & Medrano, R. . (1998). The effect of the microstructure on the superplasticity of a duplex stainless steel. *Acta Materialia, 46*(11), 3857–3862. doi:10.1016/S1359-6454(98)00087-1

Sanders, D. G., and Ramulu, M., (2004). Examination of Superplastic Forming Combined with Diffusion Bonding for Titanium: Perspective from Experience Journal of Materials Engineering and Performance 13, 744-752

Settineri, L., & Faga, M. G. (2006). Laboratory tests for performance evaluation of nanocomposite coatings for cutting tools. Wear, 260(3), 326–332. doi:10.1016/j.wear.2005.04.025

Smith, W.F., (1993). *Structure and Properties of Engineering Alloy, 2nd edition*, McGraw-Hill.

Sinha, A.K. (1991). Heat Treating. *ASM Metals Handbook, 4*, 437–447

Stein, C., Keunecke, M., Bewilogua, K., Chudoba, T., Kölker, W., & Den Berg, H. Van. (2011). Cubic boron nitride based coating systems with different interlayers for cutting inserts. *Surface and Coatings Technology*, *205*, S103–S106. doi:10.1016/j.surfcoat.2011.03.016

Superplasticity in Advanced Materials - ICSAM-2000. (2001)., *359*, 199–204. doi:10.4028/www.scientific.net/MSF.357-359.199

Tsuzaki, K., Xiaoxu, H. and Maki, T. (1996). Mechanism of dynamic continuous recrystallization during superplastic deformation in a microduplex stainless steel. *Acta Metallurgica. 44*(11). 4491-4499

Uhlmann, E., Fuentes, J. a. O., & Keunecke, M. (2009). Machining of high performance workpiece materials with CBN coated cutting tools. *Thin Solid Films*, *518*(5), 1451–1454. doi:10.1016/j.tsf.2009.09.095

Wen, J., Zhang, K., Chen, F., & Yang, Y. (2006). Activation Energy for Superplastic Flow Above Critical Temperature of Die Steels. *Journal of Iron and Steel Research, International*, *13*(5), 4–6. doi:10.1016/S1006-706X(06)60085-X

Wenbo, H., Kaifeng, Z., Guofeng, W., (2007). Superplastic forming and diffusion bonding for honeycomb structure of Ti–6Al–4V alloy, Journal of Materials Processing Technology 183, 450-454.

Xing, H. (2004). Recent development in the mechanics of superplasticity and its applications. *Journal of Materials Processing Technology*, *151*, 196–202. doi:10.1016/j.matprotec.2004.04.039

Xu, C., Gao, W., & Yang, Y. (2001). Superplastic boronizing of a low alloy steel Ð microstructural aspects, *108*, 349–355.

Xu, C. H., Xi, J. K., & Gao, W. (1997). the mechanical pr superplastic layers, *65*, 94–98.

Zealand, N. (1996). Isothermal superplastic boronizing of high carbon and low alloy steels. *Scripta Materialia*, *34*(3), 455–461.

Zelin, M. G. (1996). Processes of Microstructural Superplastic Deformation, *329*.

Internet Source :

URL: 1) http://www.metallographic.com/Newsletters/Chemical-Etching.PDF
URL: 2) http://www.xraydiffrac.com/xraydiff.html
URL: 3) http://www.nis.unito.it/lab/lab-xrd.html
URL: 4) http://www.calce.umd.edu/general/Facilities/Hardness_ad_.htm
URL: 5) http://metals.about.com/library/bldef-Vickers-Hardness-Test.htm
URL: 6) http://en.wikipedia.org/wiki/Optical_microscope